World Journal of Materials Science
ISSN: 2960-0146
DOI: https://doi.org/10.61784/wjms3004

FABRICATION OF POLYPROPYLENE NANOCOMPOSITE FOR SUPERLATIVE REFRIGERATED VEHICLE PANELS

Uwa Chukwunonso Aghaegbulam[1*], Sadiku Emmanuel Rotimi[2], Jamiru Tamba[1], Huan Zhongjie[1], Mpofu Khumbulani[3], Ramatsetse Boitumelo Innocent[3]
[1]*Department of Mechanical and Mechatronics Engineering, Tshwane University of Technology, Pretoria, South Africa.*
[2]*Institute of Nano Engineering Research and Department of Chemical, Metallurgy and Materials Engineering, Tshwane University of Technology, Pretoria, South Africa.*
[3]*Department of Industrial Engineering, Tshwane University of Technology, Pretoria, South Africa.*
Corresponding Author: Uwa Chukwunonso Aghaegbulam, Email: nonso_uwa@yahoo.com

Abstract: Refrigerated foods vehicle by road is made up of three-layered materials insulated panel that has insulation foam, situated intermediate to two high thermal conductive aluminum metal sheets. Usually, a loss of insulation value in a refrigerated vehicle every year is a result of the increase in heat absorption and heat transfer of the metal sheets, which affect the cooling temperature in a refrigerated vehicle panel chamber. The study aims at proposing the fabrication of polypropylene nanocomposite for superlative refrigerated vehicle panels, by producing and testing low-thermal conductive polymer-based composite materials with nanoclay (NC) particles for use in superlative refrigerated vehicle panels. The melt blending compounding method involved the pre-treatment of materials, preparation of composite samples, and the characterization of the new samples for their: mechanical, morphology, and thermal properties. The result of the study shows that melt blending influenced the composites' mechanical, morphology, and thermal properties. Meanwhile, the processing route exhibited an intercalated morphology structure, which enhanced the composites' strength, stiffness, and thermal conductivity. Finally, the sample with 3% nanoclay by weight had the optimum property and could be, recommended for refrigerated vehicle panel insulation.
Keywords: Polypropylene; Nanocomposite; Nanoclay; Refrigerated vehicle panels; Maleic anhydride grafted polypropylene

1 INTRODUCTION

Refrigerated vehicles are temperature-controlled vehicles, made of an insulated panel and a cooling system used to transport garden-fresh food and its products [1-2] (see Figure 1). The extension of shelf life by using the refrigerated vehicle to convey food products is important to address the growth in population. The aluminum or steel metal panel sheets used in the refrigerated panel have a high thermal conductivity which leads to high energy consumption, high engine power, decreases the longevity of the insulating materials, and causes environmental pollution. The purpose of this vehicle is to preserve the chill temperature and not to provide cooling [3].
The temperature in a refrigerated vehicle is the key parameter in sustaining the shelf-life of perishable food [4-5]. Thus far, refrigeration is one of the most broadly used techniques, to slow the bacteria growth that leads to food deterioration [6]. Suitable control of temperature is important in conveying perishable food to consumers and also to make sure they are in a good state for consumption [7]. Cooling is an active technique for reducing the growing speed of microorganisms and therefore, prolonging the shelf life of perishable foods [5]. A temperature of 4oC or lower is, considered the safe refrigeration temperature [8-9] (see Figure 1).
Refrigerated vehicles are of different sizes or types, which include: refrigerated rigid vehicles, refrigerated vans, and refrigerated semi-trailers [10-11]. These vehicles range, in weight, between 3.5-6 tons, 7.5-12 tons, 15-18 tons, and 23-26 tons [12-13].
The cooling system of refrigerated vehicles comprises the compression system, which uses power from an external power supply source, e.g., a generator or power from the vehicle's owner [14]. The compressor unit is usually located in the engine bay and the fan belt drives it. Piping links the compressor to the cooling equipment, inside the insulated chamber of the vehicle [15]. Then, the condenser unit is located either in the engine compartment or on the roof of the vehicle, where an electric standby system is fitted [16]. The mains-powered compressor is installed in the condenser compartment for use when the engine of the vehicle is not running [16].
The thermal conductivity of a refrigerated vehicle insulated panel is governed by Equation 1:

$$k_{tot} = k_s + k_g + k_r + k_{con} + k_{coup} + k_{leak} \quad (1)$$

To maintain as low thermal conductivity as possible, each of the above thermal contributions has to be minimized.

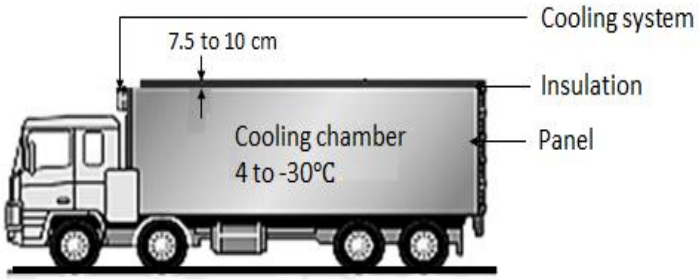

Figure 1 Image of a 7.5–12 Tons Refrigerated Vehicle [17]

The creation of composite sheets using various experimental techniques for the exterior and interior walls of refrigerated vehicles is compared. This study examined testing apparatus and the conditions for creating PPPNC composites. The practical outcomes help to clarify the findings in light of the use of the proposed refrigerated vehicle panel. The study introduces a novel energy-saving technique for refrigerated food transportation that, at the time this study was being conducted, had not yet been covered by any previous publications.

The longevity of the insulating material in refrigerated vehicles will also be impacted by conventional insulation panels, which are made of metal and have high thermal conductivities that result in significant energy usage. This brings up financial and environmental concerns. The rate at which heat is transferred into the refrigerated compartment through the wall layers determines the thickness of the insulation material [19]. However, because trailers and vehicles have fixed outside dimensions, the thickness of insulation material also reduces freight space. Typically, 0.026 W/m°C low thermal conductivity urethane foam is utilized as an insulating material in the sandwich panel of a refrigerated vehicle [20]. The most often used insulation is a core made of expanded polyurethane (PU) foam [21]. The insulation materials used in refrigerated vehicles, together with their thermal conductivity (K) values, advantages and disadvantages, are listed in Table 1.

Table 1 Insulating Materials, K Values, Benefits, and Drawbacks [18-21]

Materials	Thermal conductivity (mW/mK)	Advantages	Disadvantages
Aerogel	4 (at 13 ambient pressure)	1). It offers excellent insulation 2). It has great compression strength	1). It is more expensive 2). It is also quite delicate due to its poor tensile strength
Fibre glass	16-26	1). It is affordable	1). It needs to be handled carefully
Cork	40-50	1). It serves as a board or filler material	1). It is not fireproof
Mineral wool	30-40	1). It is soft and light 2). It is efficient	1). It is not resistant to fire. 2). K value increases with moisture content, temperature, and the mass density increases from 37-55 mW/mK
Cellulose	40-50	1). It is fire resistant 2). It is Eco-friendly 3). It is effective	1). It is difficult to application 2). K value increases with moisture content, temperature, and the mass density increases from 40-66mW/mK
Polystyrene	30-40	1). It functions as a variety of insulation materials	1). Its safety is in question 2). It possesses an open pore structure 3). K value increases with moisture content, temperature, and the mass density increases from 30-65 mW/mK
Polyurethane	20-30	1). Generally excellent insulating product	1). It is not eco-friendly 2). K value increases with increasing moisture content from 25-45 mW/m.K from 0 vol% -10 vol%

Vacuum insulation panels (VIPs)	3-4 and 8 (fresh condition)	1). It has longevity of 25years	1). It has a high cost 2). Its k values are in the range of 5 to 10 times 3). Age can cause it to deteriorate 3). VIPs have a lesser heat resistance than traditional insulating materials like mineral wool and polystyrene
Gas-filled panels (GFPs)	40	1). It has a lifespan of 25years	1). It has a high cost 2). Its K value is in the range of 5 to 10 times which is dependent on the ageing period. GFPs are lower than mineral wool, and polystyrene
Phase change materials	19	1). Thermal insulating materials that really work	1). Heat phase change is affected from the transition of a liquid into a solid

To create polymer/clay nanocomposites, many blend techniques have been explored. In-situ intercalative polymerization, melt intercalation, solution intercalation, and template syntheses are the four manufacturing techniques often used for nanocomposites [22-26]; however, melt intercalation was the approach employed in this study. Because it is currently the best scalable technology for industrial application, the melt intercalation technique with Haake Rheomixer OS was chosen for this investigation. Also inexpensive and environmentally benign is the melt intercalation processing method. For polypropylene/nanoclay composites, melt intercalation is advantageous. Table 2 below illustrates the processing techniques for polymer nanocomposites as well as their benefits and drawbacks.

Table 2 Processing Methods, Advantages, and Disadvantages of Polymer Nanocomposites [22-26]

Processing methods	Advantages	Disadvantages
Pre-polymer/ Intercalation from solution	1). For the blend of intercalation polymers nanocomposites with low or no polarity. 2). For the fabrication of similar dispersals of fillers.	1). The industries employ significant volumes of solvents.
In-situ Intercalative Polymerization	1). Considering the filler's dispersion in the polymer precursors, the procedure is simple.	1). Controlling intra-gallery polymerization is challenging. 2). The number of applications is small.
Melt Intercalation	1). When compared to other techniques, this is the fabrication process for polymers that works the best. 2). It is safe for the environment. 3). It works well for manufacturing industrial polymers.	1). Its utilization is restricted to polyolefin, which makes up the majority of common polymers.
Template Synthesis	1). It is used for massive production. 2). The processing steps are simple.	1). It only has a few uses. 2). It mainly focuses on polymers that are soluble in water. 3). It is contaminated with side products.
Sol-Gel Process	1). It is an easy technique. 2). It requires a low processing temperature. 3). It has many uses. 4). It has good chemical homogeneity. 5). Its stoichiometry mechanism is comprehensive. 6). The purity of its products is high. 7). It is applied to the creation of metal-oxygen-based 3-dimensional polymers. 8). Both singles and matrices can be processed with it. 9). The production of composite materials using liquids or sticky fluids made from alkoxides is a particular application for which it is suitable.	1). Compared to the mixing process, it has a higher shrinkage and fewer voids.

The paper aims to fabricate low-thermal conductive polymer-based composite materials for use in superlative refrigerated vehicle panels using the melt-blending processing method. This will reduce fuel consumption rate, payload, engine power, and environmental effect.

2 NANOCOMPOSITES

2.1 Review of Polymer Nanocomposites Application in Automobile

Weight reduction and insulation in automobiles can be achieved with the use of polymers [27]. These polymeric materials can reduce engine power, carbon emission, and energy consumption. Polymers used in automobiles can be classified based on their applications, namely: polymers for weight reduction, high-performance polymers, reinforced polymers, polymer/metal hybrid systems, and polymers sandwich panels [28]. Table 3, displays the different types of polymers used in automobiles and the areas of application.

General Motors (GM) has used nanocomposites in the commercial auto exterior to assist on the 2002 General Motors Commercial and Passengers Safari, and Chevrolet Astro vans and in the 2003 and 2004 models [29]. GM also used PP/nanoclay composite, appearing in the body side molding of the highest-volume car, the 2004 Chevrolet Impala [30-31]. The compound was, developed by the GM's Research and Development Center in Warren, Michigan, in cooperation with Basell North America and Southern Clay Products [32]. The most recent application of nanocomposite is on the 2005 GM Hummer H2 Sport Utility Truck (SUT). This vehicle's cargo bed uses about seven pounds of molded-in-color nanocomposite parts for its box-rail protector, sail panel, and center-bridge [33]. Furthermore, the material used on the GM Hummer H2 SUT is the Basell's Profax CX-284 reactor Thermoplastic Polyolefin with nanoclay [34]. Additionally, nanoclay adds muscle to plastics, while carbon nanotubes impart electrical and thermal conductivity [35]. However, almost every car produced in the United States, since the late 1990s, contains some carbon nanotubes, typically blended into nylon in order to protect against static electricity in the fuel system [36].

PP has been applied in the following areas of automobiles: electrical components, exterior trim, lighting, bumpers, hood components, interior trim, upholstery, seats, dashboards, fuel systems, body panels, and other reservoirs [37-38] (see Table 4).

Table 3 Summary of Polymers, Properties, and the Areas of Applications in Automobiles [39-43]

Name of polymer/matrix	Properties of polymer	Application in automobile
Polyetheretherketone	Chemical resistant, good friction wear properties and heat-resistant.	Brake parts, oil pump, ball joint, washer, transmission parts, and bearing.
Polybutyleneterephthalate	Dimensional accuracy, heat resistant, good electrical insulating, and rigid.	Connector housing, bumper coverings, exterior auto body parts, electronic housings, and plugs.
Polymethylmethacrylate	Scratch-resistant, stress-cracking-resistant, ultraviolet resistant, and transparent.	Rear lamps and headlight lenses for blinker.
Polyethyleneterephthalate	Rigid, Tensile strength, and good barrier effect.	Airbags, coverings, textiles, and seat belts.
Acrylonitrile Butadiene Styrene Copolymer	Solid, dimensionally stable, and electroplatable.	Dashboard, interior panelling, radiator grills, and wheel Panels.
Polyoxymethylene	Thermally stable, abrasion-resistant, low tendency to creeping, impact-resistant, and chemical resistance	Bearing components, connectors, and clips.
Polyvinylchloride	Low cost, weather-resistant, good haptic, and non-inflammable.	Cable insulation, protective bordering, underbody protection, and interior panelling.
Polyamide	Rigid, temperature-stable, aging-resistance, low gas permeability, and permanent solid.	Connector housing, wheel panels, plugs, motor covering, suction elbows, mirror housing, and door handles.
Polyethylene	Low cost, chemical resistance, good solidity, and, aging-resistance.	Fluid containers, windshields, and fuel tanks.
Polycarbonate	Impact-resistant, transparent, and ultraviolet resistant.	Exterior auto body parts, tail light cover, headlight lenses, and bumper coverings.
Polyurethane	Damping, good elasticity, and low heat conductivity.	Exterior elements, dashboard, seat upholstery, and roof padding.
Polypropylene	Chemical resistance, good solidity, and low-cost.	Crash panel, wheel housings, guide channels, containers, side panels, air filter housings, door trim,

battery case, seats, and bumpers.

2.2 Review of Nanocomposites Based Matrix

Polymer matrix nanocomposites are the blend of polymer and nanocomposites which show some potential in insulating materials manufacturing because of their promising properties which can be obtained with very low filler content [44-45]. As well known, the performance enhancement of these composites is realized when clay particles are accurately dispersed in the polymer matrix and intercalation between matrix macromolecules and clay lamellae exists [46-47].
Nanofillers are normally classified into three geometries namely; rod or fiber-like, equi-axial or particles, and sheet [48-49]. An important advantage of small-sized particles is the high surface-to-volume ratio which is varied by the particle geometry. Properties of polymer nanocomposites can be attributed to the type of nano-scale fillers used in the composite. Many types of nanofillers like carbon, clay, aluminum oxide, and silica are commercially available today but clay or Montmorillonite (MMT) is one of the most studied in polymer nanocomposites [50-51].
Nanoclays simply become “nano” when they are placed in a host polymer matrix, whereupon they cannot be distinguished or separated from the bulk polymer and other constituents [52-53]. Nanoclays, inclusive of their primary function as high aspect ratio reinforcements, have significant functions such as synergistic flame retardant, barrier, and thermal properties. Some of the factors responsible for good performance in nanocomposites are exfoliation (involve dispersion and delaminating); interfacial adhesion or wetting; and intercalation (involves surfactant and polymer) [54-58].
PP, which is a polyolefin polymer type, is considered one of the most widely used thermoplastic materials in the plastics industry [59]. A well-developed PP/clay nanocomposite has a great potential of being, applied in diverse areas of industry, such as packaging, bottle, automobile, and film, etc., [60-62]. However, because of the non-polar nature of polypropylene, it is difficult to exfoliate clay layers and to have homogeneous dispersion of the clay layers in the PP matrix [63]. This is because the organophilic clays have polar hydroxyl groups and are compatible only with polymers containing polar functional groups [64]. In order to resolve the incompatibility between no polar polymer and polar clay, compatibilizers, such as maleic anhydride grafted polypropylene (PP-*g*-MA) and the hydroxyl groups’ grafted polypropylene, are used [65-67]. The compatibilizer contains polar functional groups, which enhance the interface interaction between the PP matrix and the clay [68-72].

Table 4 Summary of Materials and Their Nanocomposites Properties [73-75]

Material	Features	limitation	Nanocomposites of the material based on matrix	Advantages of nanocomposites
Metal	Ductile, toughness with high strength and modulus, electrical and heat conductivity.	Highly corrosive	Metal matrix nanocomposites (MMNC).	High strength in shear or compression processes, high electrical and thermal stability, wear, and chemical resistance.
Ceramic	Good wear resistance and high thermal and chemical stability.	They are brittle or low toughness	Ceramic matrix nanocomposites (CMNC)	Enhanced mechanical properties including fracture toughness, stiffness, and strength due to the crack bridging role of nanofillers. Ceramic in matrix nanocomposites offer striking magnetic, electronic, optical, or catalytic properties, and dramatic improvement in biodegradability.
Polymer	Widely used in industry due to its ease of production, lightweight, and ductility.	Low modulus and strength.	Polymer matrix composites (PMNC)	Polymers or inorganic compounds increase heat and impact resistance, flame retardant, and mechanical strength and decrease gas permeability with respect to oxygen and water vapor. Polymer/metal or ceramic offers striking magnetic, electronic, optical, or catalytic properties, and dramatic improvement in biodegradability.

Consequently, the objective of this work is to produce a low thermal conductive polypropylene nanocomposite for use as an insulator in superlative refrigerated vehicle panels with the purpose to reduce consumption, engine power, and weight; although retaining the other characteristic properties of the existing panel materials. PP, NC, and MA-*g*-PP are the materials used in this study.

2.3 Methodology for Nanocomposites Preparation

For the enhancement of a specific matrix material property, for example, the increase in the matrices' electrical, mechanical or optical properties, it is useful to have the nano particulates evenly dispersed in the matrix [76]. Accomplishing a suitable dispersion can be a challenging task due to the Van der Waal forces existing between the nano additives that cause agglomeration of the nanoparticles [76]. In order to obtain a suitable dispersion of such additives, a variety of methods, have been studied and adopted over the years and the outcomes are, documented in the literature [76]. The conventional preparation methodologies of nanocomposites are, explained in three different schemes, as shown in Figure 2 Scheme II methodology was, used in this study to prepare polypropylene nanocomposite for use in a superlative refrigerated vehicle insulated panel.

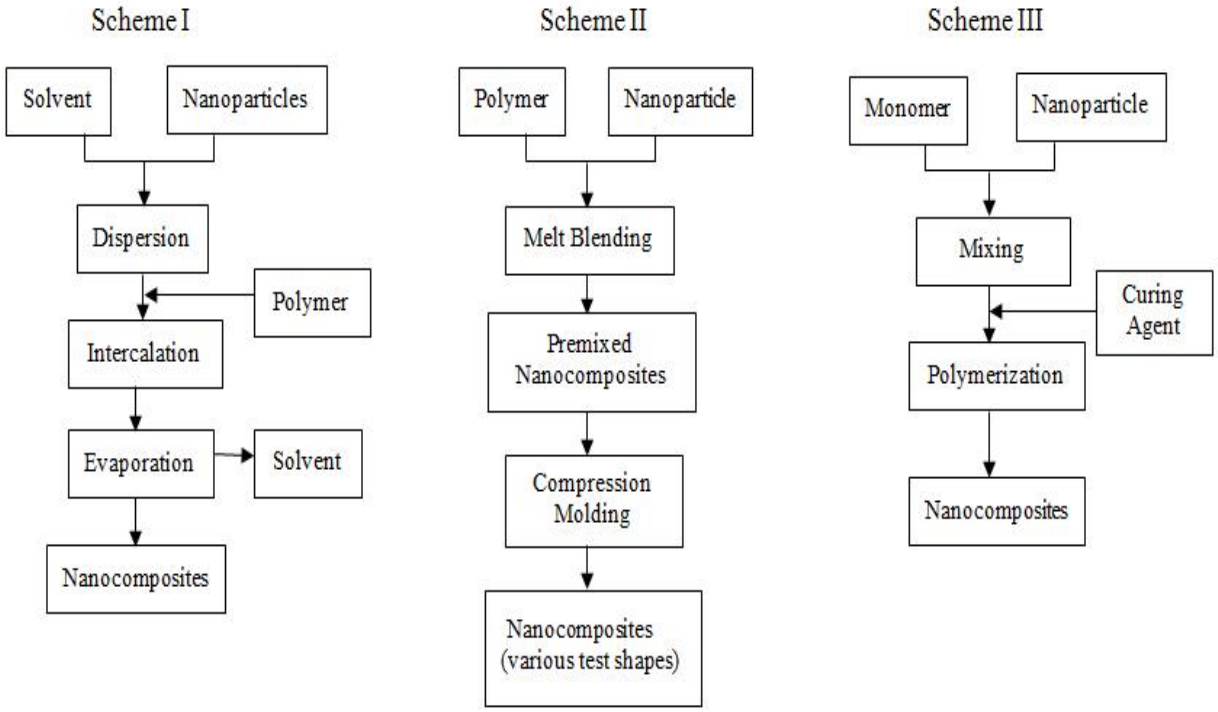

Figure 2 Methodologies for Common Nanocomposites Preparation [76]

3 EXPERIMENTAL

3.1 Materials

The polypropylene impact copolymer CPV340 was produced by Sasol Polymers Product South Africa, and has the following specifications: Melt Flow Rate (MFR) of 16 g/10min, test condition of 230°C, 2.16kg, density of 0.905 g/m^3, tensile strength of 140 MPa, and Charpy notched impact strength of 6 KJ/m^2 at 23°C.
EastmanTM G-3003, a maleic anhydride-grafted polypropylene with this designation, was purchased from Southern Clay Products in the USA. With an ASTMD 5 standard penetration of less than 1 dmm, an MA of 5%, an acid number of 9 mg KOH/g, and a softening temperature of 180 DSC Tm °C.
Eastman Chemical Company, USA, provided the nanoclay Cloisite® 20A, with the following specifications: density of 1.77 g/cc, 8% elongation, modulus of elasticity of 4.657 GPa, amount of modifier 38%, ultimate tensile strength of 101 MPa, and inter-gallery d-spacing of 24.2. The Cloisite 20A Nanoclay type was chosen above the Cloisite Na+, Cloisite 93A, and Cloisite 30B Nanoclay kinds because it has greater property improvements and a better miscibility with polypropylene [77].

3.2 Experimental Process

The NC Cloisite® 20A grade and MA-*g*-PP G-3003 materials were pre-treated before preparation with PP CPV340 type (see Figure 3a). Melt blending compounding methodology was used in the study with a Haake Polylab rheomixer because it is environmentally friendly, and economic. Additionally, a rheomixer compounding device was used in order to ensure even

and homogeneous dispersion of the nanoclay in the resulting composites; this makes it different from the conventional processing methods that have limitations, such as weak bonding, shrinkage, agglomeration, low wearing resistance, high permeability, difficult control of porosity and voids [78].

3.3 Pre-treatment of Materials

NC and MA-*g*-PP were dried overnight in a vacuum oven at a set temperature of 80°C. This is because they are hydrophilic in nature and the process assisted in removing moisture and keeps them at their superlative conditions with increasing bonding effectiveness (see Figure 3b).

3.4 Preparation of Composite Samples

A sample of pure PP was prepared as the master batch for reference, followed by batches of samples with PP, NC, and MAPP at varying concentrations. PP was weighed into the rheomixer for two minutes to allow the material to melt after which, NC, and MA-g-PP were introduced and allowed to blend for 6min. A total mass of 50g was weighed into the rheomixer, a product of Thermo Electron Cooperation, USA (See Figure 3c). The rheomixer was operated at a rotor speed of 60 rpm and at a temperature of 190°C for the 8min mixing time for all the batches. Six sets of samples were used. Sample 1 was polypropylene (pure PP) impact copolymer as the control sample. Sample 2, Sample 3, Sample 4, Sample 5, and Sample 6, were nanocomposites with a composition of 1wt%, 3wt%, 5wt%, 7wt%, and 10wt% nanoclay by weight, respectively (see Table 5). Furthermore, the premixed samples were compression-molded with a Carver laboratory press (Model–3851-0, USA) at a pressure of 1500 psi and a temperature of 190°C for a period of 10 minutes after which, it was allowed to cure (see Figure 3d and Figure 3e). The test specimen was prepared for mechanical, morphology, and thermal characterizations according to the various standards required (see Figure 3f). The types of equipment used in Figures 3b, 3c, and 3d, are in good operating order because they are brand new, calibrated according to specifications, and are operated by competent experts.

The mixing phenomenon of the PP, NC, and MA-g-PP blends followed the theoretical mixing theory. Meanwhile, the thermodynamics of a mixture can be used to understand the principle of mixing one component with another. Gibb's free energy of mixing theory states that mixing of two or more components is favorably provided the free energy value of mixing is negative, (see Equation 2).

$$G_{mix} = \Delta H_{mix} - T\Delta S_{mix} \tag{2}$$

A negative value of the free energy shows that the mixing process is effective. Gibb's free energy of mixing was defined for the gaseous state. Later, Flory–Huggins modified Gibb's free energy for the polymer system. The general expression of the Flory–Huggins theory for the free energy of PP/NC/MA-g-PP systems is given as shown in Equations 3 and 4 below:

$$\Phi_A = \frac{n_A M_A}{n_A M_A + n_B M_B + n_C M_C}; \Phi_B = \frac{n_B M_B}{n_A M_A + n_B M_B + n_C M_C}; \Phi_A = \frac{n_B M_B}{n_A M_A + n_B M_B + n_C M_C} \tag{3}$$

$$\left[\frac{\Delta G_{mix}}{RT}\right] = \frac{\Phi_A}{M_A} In\Phi_A + \frac{\Phi_B}{M_B} In\Phi_B + \frac{\Phi_C}{M_C} In\Phi_C + \chi_{ABC}\Phi_A\Phi_B\Phi_C \tag{4}$$

The following density formula was used to determine the density values for the composites:

$$\text{Density, } \rho\ (\text{g/cm}^3) = \frac{\text{mass (g)}}{\text{volume (cm}^3)} \tag{5}$$

Table 5 Composition and Proportion of Test Samples by Weight

Sample	PP (wt%) (Matrix)	MA-g-PP (wt%) (Compatibilizer)	NC (wt%) (Reinforcement)	PP/ MA-g-PP/ NC (Blend)	Amount of PP (grams)	Density (g/cm^3)
Pure PP	100	0	0	100/0/0	50	0.857
PPNC1	95	4	1	95/4/1	49.4	0.886
PPNC3	93	4	3	93/4/3	48.6	0.893
PPNC4	91	4	5	91/4/5	45.8	0.906
PPNC5	89	4	7	89/4/7	44.3	0.913
PPNC6	86	4	10	86/4/10	41.6	0.921

Figure 3 Image of Methodology Processes: (a) Raw Materials, (b) Oven Dryer, (c) Rheomixer, (d) Compression Mold, (e) Premixed Sample, and (f) Molded-Shaped Samples

3.5 Characterization

In order to obtain shapes, sizes of the interactive surfaces, crystallinity, thermal conductivities, compositions, microstructure, orientations, intercalation, and dispersion of nanoparticles in matrices of the polymer, the appropriate characterization of the materials produced was carried out with suitable techniques and specifications. The sample requirements, such as thermal conductivity, mechanical tensile, and physical qualities (morphology: F-TIR, SEM, and X-ray), were demonstrated by accepted foundations such the American Society for Testing and Materials using accepted test procedures (ASTM).

The tensile strength and modulus or stiffness of the samples were determined by using the Instron 5966 tester (Instron Engineering Corporation, USA), with a load cell of 10 KN, by ASTM D638. The morphology of the test samples was also examined with the Scanning electron microscope (JEOL JSM-7500F, Germany) instrument with an accelerating voltage of 15Kv. Wide-angle X-ray diffraction (WAXD), PanAnalytical Xpert Pro diffractometer, (The Netherlands), using a CuK radiation with a wavelength of 0.154 nm at a voltage of 45 kV and a current of 40 mA, was used to study the crystalline structures of all the samples and nanoparticles as well as the pure polypropylene used as a reference. Both organic and inorganic samples were identified and described using Fourier Transfer Infrared Spectroscopy (FTIS). It recognized the molecules' chemical linkages. Fourier transfer infrared (FTIR) spectroscopy was used on the samples with a PerkinElmer Spectrum 100 FT-IR spectrometer in the wavelength range of between 500 and 4000 cm/sec-1 to determine the existence of any chemical interactions between PP, nanoclay, and MAPP. The IR absorption spectrum, which corresponds to the bands existing in the chemical substance and distinctive functional group, is produced when the molecules of chemical substances vibrate and cause selective absorption in the infrared (IR) region, as shown in FTIR analysis images.

Rectangular samples were prepared with dimensions of 10mm x 4mm. The in-plane and through-plane thermal diffusivity (a), were determined by using a laser flash method on Netzsch LFA 427 SOP instruments. Nitrogen was, used to stabilize the temperature or cooling in the furnace and argon gas was for the atmosphere inside the furnace. Processing conditions: set temperature range of between 25°C–100°C, laser voltage 450v, pulse width 0.8ms, Atmosphere-Argon gas and flow rate 100ml/min, heating rate 50k/min, and time distance 1min. The LFA 427 instruments were operated following ASTM E1461 and ISO 18755 standards. The thermal conductivity of the samples was, calculated by using the formula in Equation 6:

$$k = \alpha \,.\, C_P \,.\, \rho \tag{6}$$

4 RESULTS AND DISCUSSION

The tensile tests results showed increases in strength and modulus of the nanocomposites when compared to the pure PP (see Figure 4). The composite sample with 3 wt% clay content gave the best mechanical property in terms of strength and stiffness, as shown in Figure 4a and Figure 4b. This is attributed to the bonding effect of the MAPP in the mixture of PP and NC.

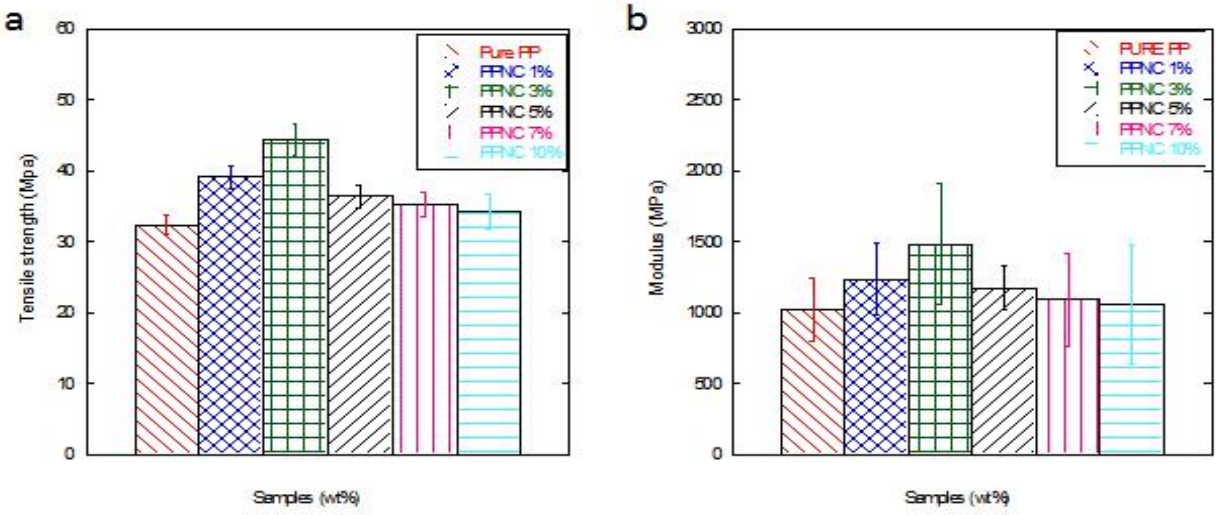

Figure 4 Plots of (a) Tensile Strength and (b) Tensile Modulus as Functions of Nanoparticles wt% Inclusion

The Scanning electron microscope (SEM) micrographs, as shown in Figure 5, display the degree of PP chains penetration into the NC gallery. Intercalated structures were observed in the morphology of the samples. The use of rheomixer adequately dispersed the NC filler evenly in the matrix of PP (see Figure 5). The homogenous dispersion of clay in the PP matrix enhanced the strength and modulus of the nanocomposites when compared to the pure PP (see Figure 4). At 1wt%, 3wt%, and 5wt% clay contents, the homogenous dispersion of clay was observed, but as the NC inclusion in the PP matrix increased, the crack was initiated in 7wt% clay content. Then, when it got to 10wt% clay content, fracture propagation was noticed. SEM micrograph corresponds to the rise and fall in the strength and modulus of the samples, as shown in Figure 4a and Figure 4b.

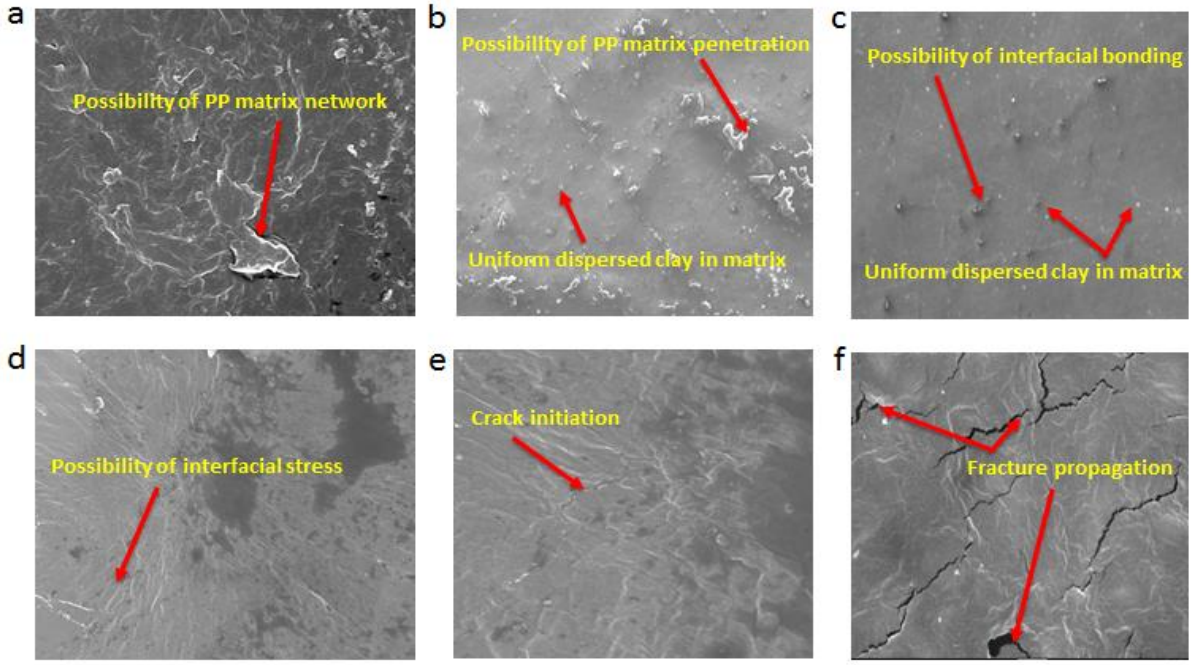

Figure 5 SEM Micrographs of: (a) Pure PP, (b) PPNC 1%, (c) PPNC 3%, (d) PPNC 5%, (e) PPNC 7% and (f) PPNC 10%

To identify the different forms of bonding in the composites, FT-IR analysis of the PPNC composites was performed. The various chemical linkages that have formed as a result of the treatment and curing of composite materials were shown by the FT-IR spectra in Figure 6. Peaks demonstrate significant absorption and low transmittance. As we move to the left, the wavenumber on the horizontal axis rises. The regions with no peaks show photons that have not been absorbed at that frequency, indicating that the molecule does not contain the particular bond at that frequency [79]. The functional groups C=O, -OH, CH, CH2, and CH3 are responsible for the absorption bands in the 4000-500 wave number range [80-81]. The region between 300 and 500 is referred to as the "fingerprint region," and it results from intermolecular interactions unique to each substance. Infrared light is not absorbed by any bonds since pure PP is homogeneous and does not bond with any other substance. In Pure PP, there is no bond vibration to produce absorption bands. Figure 4.4 depicts endothermic peaks, whereas PPNC 3wt% showed an exothermic peak at peak 1025, which may be the reason for PPNC 3wt%'s superior mechanical properties in terms of strength and stiffness.

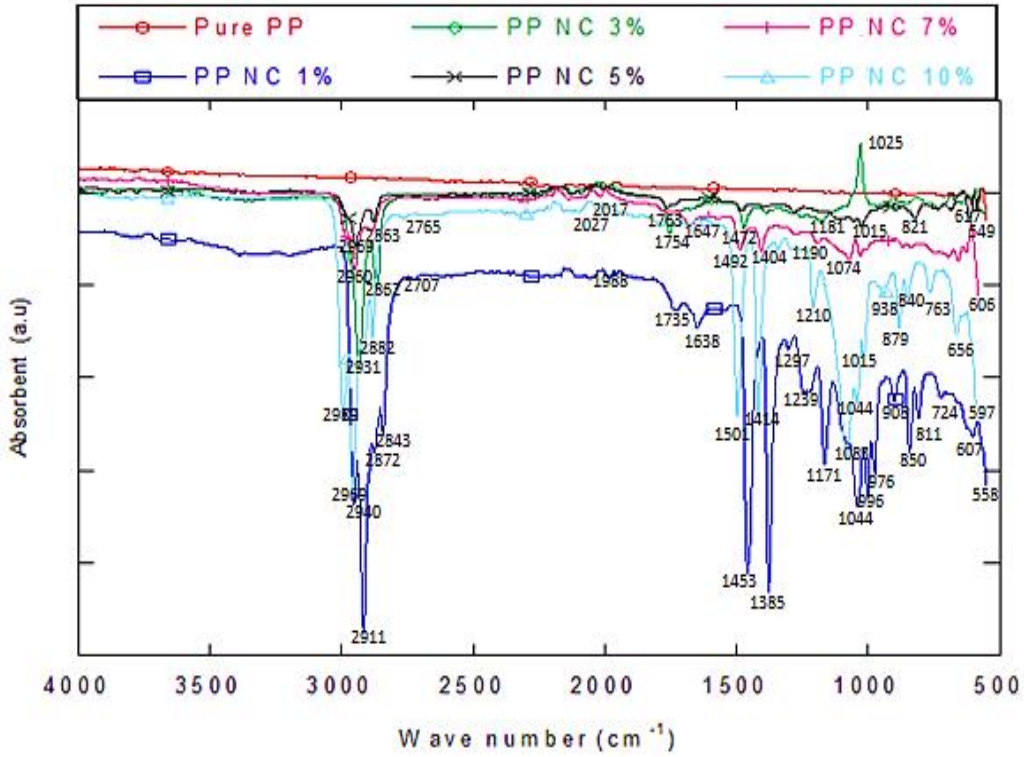

Figure 6 FT-IR Spectra of Pure PP and Nanoclay-Based PP Composites with MA-g-PP [82]

Table 6, lists the important infrared (FT-IR) bands and associated functional groups that were allocated to PPNC composite samples.

Table 6 PP Segment Absorption Bands in the Infrared on MA-g-PP and NC [83-85]

Peak	Peak Assignment
811	C-C stretch, CH2 rock, C-CH stretch
850	OH bend
908	C-CH_3 stretch, CH_2 rock
996	C-C stretch, CH_3 rock
1044	CH_3 bend, CH_3 rock, CH bend
1171	CH_3 rock, CH bend, C-C stretch
1297	CH bend or Aromatic ring stretch
1385	CH_2 bend, C-O stretch
1453	C=O stretch, CH_2 bend
2843	C-H stretch
2911	C-H stretch

2940 C-H stretch

The addition of compatibilizer and nanofiller to PP matrix resulted in intercalated structures, as shown by XRD examination [86].

The intercalated structures seen in the SEM micrographs are further supported by the XRD analyses. However, as the inter-planer d-spacing increased% content, as demonstrated in SEM micrographs, XRD diffraction demonstrates the peaks relate to intercalation. This shows that as clay is loaded into the matrix, intercalation causes the interlaying gaps to shrink, which has an impact on the samples' density and thermal conductivity (see Figure 8). When polymer chains are intercalated, there is a change in the peak's diffraction angle, which corresponds to a change in the interlayer molecules' d-spacing of the composites in Figure 7 [87].

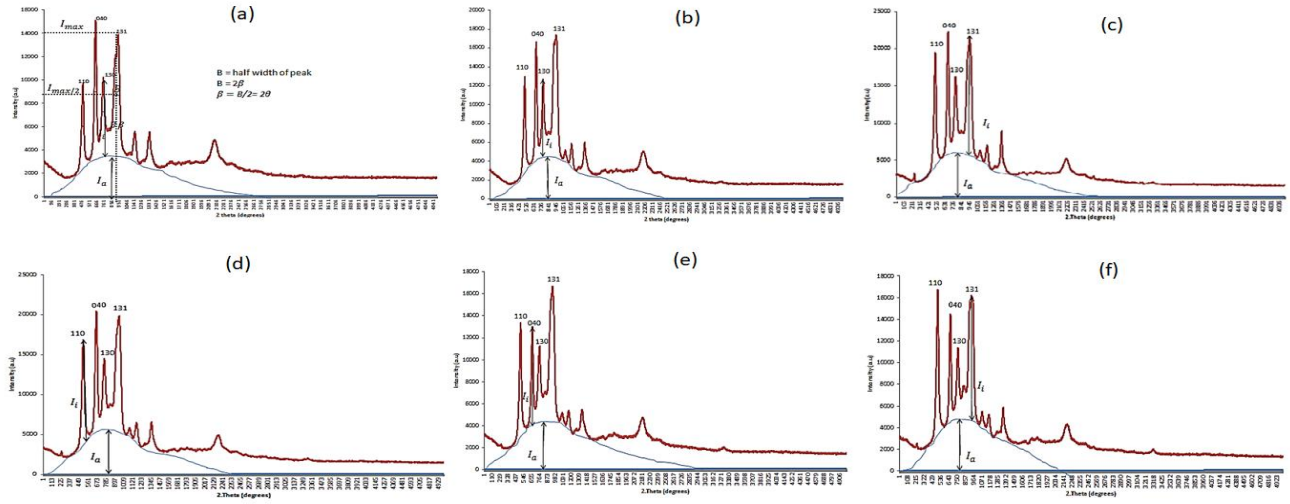

Figure 7 XRD diffractogram of Pure PP, PPNC1, PPNC3, PPNC5, PPNC7, and PPNC10 [88]

Scherrer's equation, which is shown in Equation 7, and it is used to compute the crystallite sizes in the samples, is displayed in Table 7 below:

$$\text{Size of Crystal } (L_c) = \frac{K\lambda}{\beta\cos\theta} \tag{7}$$

Where:

L_c = size of the crystallites (in nm), measured parallel to the crystallographic plane

k = 0.89 (constant)

= utilized wavelength ($\lambda_{CuK\alpha} = 1.54\text{Å or } 1.54\text{nm}$)

θ = diffraction angle

β = half-weight of the peak in regard to the crystallographic plane, expressed as hkl (in radian)

Table 7 Samples' Crystallite Sizes

Sample	Size of a crystallite (nm)			
	$I_{(110)}$	$I_{(040)}$	$I_{(130)}$	$I_{(131)}$
Pure PP	0.3197	0.2284	0.2008	0.1553
PPNC1	0.3116	0.2092	0.1819	0.1489
PPNC3	0.3092	0.2086	0.1821	0.1489
PPNC5	0.2923	0.2147	0.1993	0.1503
PPNC7	0.2993	0.2213	0.2044	0.1522
PPNC10	0.3017	0.2251	0.2088	0.1555

When compared to pure PP, Table 7 shows that the crystallite diameters of peak 110 shrank with increasing clay content, which suggests that clay may have intercalated into the polypropylene matrix in the presence of the compatibilizer, maleic anhydride-grafted polypropylene. More importantly, it is thought that the presence of clay slowed the growth of PP crystals during crystallization, resulting in smaller crystal sizes. When compared to a reference sample of pure PP, it was found that the size of the crystallite reduced at low clay loading and grew at high clay loading. This might be due to the weak compatibilizer that was utilized to combine the components, a parameter that was maintained throughout.

The thermal conductivity of the samples reduced as the clay contents increased, as shown in Figure 8. The thermal conductivity of the composites is dependent on the macromolecular size, molecular weight distribution, degree of crystallinity, amount of clay in the composite, and crystallite orientation. The composite sample with 10wt% clay content, had the lowest value of thermal conductivity, which is the best value obtained for the thermal conductivity, it, however, failed in strength, as shown in Figure 4. Therefore, the 10wt% composite is not suitable for refrigerated vehicle panel insulation.

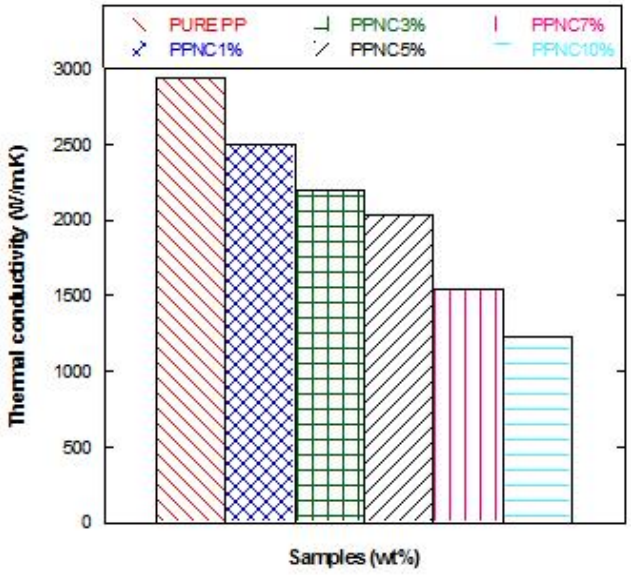

Figure 8 The Plot of Samples' thermal conductivity

5 CONCLUSIONS

PP nanocomposite, which offers new technology in automobile and food storage industries, as well as being environmentally friendly, is a good applicant of sustainability that has its indicator on the environment, social, and economy. Isotactic polypropylene composites' morphology, strength, stiffness, physical, and thermal properties were all enhanced by the addition of nanoclay. Characterization results of pure PP and PPNC composites showed that changes to these samples' compositions or microstructures would have an impact on their weights and thermal conductivities. When clay was loaded into the PP matrix at low levels (PPNC1 and PPNC3), both the tensile strength and the Young's modulus rose, but they decreased at higher levels (PPNC5). It becomes apparent from this that an increase in strength may be connected to interaction. The study showed that the tensile strength and modulus of PP nanocomposites were improved due to the strong interface bonds between the matrix and the dispersed phase. The low thermal conductivity properties of PP nanocomposites were, related to the processing methodology, which ensured uniform dispersion of NC in the PP matrix with the help of MA-*g*-PP as the compatibilizer. PPNC 3 gave the best desirable property since strength and stiffness are important in selecting a composite for the superlative refrigerated vehicle insulation panels' application.

The comparatively high level of crystallinity detected in XRD may be responsible for the rise in modulus. PP nanocomposites' XRD diffractograms revealed an intercalation structure, however at loadings of 7wt% and 10%, clay particles clumped together. SEM micrographs demonstrated acceptable clay dispersion at low clay contents (1 wt and 3 wt%) but poor dispersion and massive agglomerates at higher clay contents (7 wt% and 10 wt%). By absorbing infrared light, the samples' molecules vibrated, producing endothermic peaks in their FTIR spectra. The best quality was displayed by PPNC3. According to a thermal conductivity analysis, PPNC composites' thermal conductivity decreased as clay loading in the PP matrix increased. The mechanical qualities are enhanced during preparation by properly scattered clay in the PP matrix. Due to the appropriate distribution of nanoclay on PP matrix, PPNC composites demonstrated the highest thermal resistance properties. The endothermic effect influences thermal degradation of pure PP, which started before mass loss began. In contrast, in nanocomposites based on nanoclay, the endothermic effect was completely diminished, and thermal degradation shifted towards higher temperatures and was connected with mass loss.

The study revealed that nanoclay-reinforced polypropylene matrix possessed excellent performance-insulating properties and might assist the construction of refrigerated vehicles in lowering weight, reducing thermal conductivity, and protecting the environment from CO2 emissions. In a refrigerated panel wall application, PPNC3 is suggested as an alternative to steel

or aluminum. However, more research is necessary before choosing the best values for nanoclay. The study's findings supported the idea that adding nanoclay improves the morphological, mechanical, and thermal resistance qualities of PP. However, more research is necessary before choosing the best values for nanoclay.

LIST OF ABBREVIATIONS

PP	Polypropylene
NC	Nanoclay
MA-g-PP	Maleic anhydride grafted polypropylene
MMNC	Metal matrix nanocomposites
CMNC	Ceramic matrix nanocomposites
PMNC	Polymer matrix nanocomposites
ΔH_{mix}	Change in enthalpy of mixing
G_{mix}	Gibb's free energy of mixing
ΔH_{mix}	Change in enthalpy of mixing
ΔS_{mix}	Entropy of mixing
T	Absolute temperature
M_A	Molar fraction of PP
M_B	Molar fractions of NC
M_C	Molar fractions of MAPP
n_A	Molecules number of PP
n_B	Molecules number of NC
n_C	Molecules number of MAPP
Φ_A	Volume fraction of PP
Φ_B	Volume fraction of NC
Φ_C	Volume fraction of MAPP
X_{ABC}	Flory-Huggins interaction parameter of three components in the mixture
k_{tot}	Total thermal conductivity
k_s	Solid state thermal conductivity
k_g	Gas molecule's thermal conductivity
k_r	Radiation thermal conductivity
k_{con}	Convection thermal conductivity
k_{coup}	Thermal conductivity of thermal conductivities interface
k_{leak}	Leakage thermal conductivity
α	Thermal diffusivity (cm^2/s)
k	Thermal conductivity (W/mK)
ρ	Density (g/cm^3)
C_p	Specific heat capacity (J/K)
In	Natural logarithm
R	Gas constant
MPa	Megapascal
GM	General motors
MMT	Montmorillonite
USA	United States of America
SEM	Scanning Electron Microscope
SUT	Sport Utility Truck

COMPETING INTERESTS

The authors have no relevant financial or non-financial interests to disclose.

AVAILABILITY OF DATA AND MATERIAL

Data sharing does not apply to this article as no datasets were generated or analysed during the current study.

AUTHORS' CONTRIBUTIONS

T designed the work. Z contributed largely to the conception. CA carried out the experimental studies. ER analysed the experimental data. K edited the work. BI revised the work.

ACKNOWLEDGMENTS

The authors would like to express their thanks to the Tshwane University of Technology (TUT) Pretoria, South Africa for providing a favourable research environment and the Institute for Nano-Engineering Research Laboratory (INER), TUT, where some of the experiments were carried out. Furthermore, the CSIR Centre for Nano-structured Materials' assistance in carrying out the successful tests and analyses is gratefully acknowledged.

REFERENCES

[1] Neri L, Faieta M, Di Mattia C, et al. Antioxidant activity in frozen plant foods: Effect of cryoprotectants, freezing process and frozen storage. Foods. 2020, 9(12): 1886.
[2] De Corato U. Improving the shelf-life and quality of fresh and minimally-processed fruits and vegetables for a modern food industry: A comprehensive critical review from the traditional technologies into the most promising advancements. Critical Reviews in Food Science and Nutrition, 2020, 60(6): 940-75.
[3] Adekomaya O, Jamiru T, Sadiku R, et al. Minimizing energy consumption in refrigerated vehicles through alternative external wall. Renewable and Sustainable Energy Reviews, 2017, 67: 89-93.
[4] Kuo JC, Chen MC. Developing an advanced multi-temperature joint distribution system for the food cold chain. Food control, 2010, 21(4): 559-66.
[5] Glouannec P, Michel B, Delamarre G, et al. Experimental and numerical study of heat transfer across insulation wall of a refrigerated integral panel van. Applied Thermal Engineering, 2014, 73(1): 196-204.
[6] Aung MM, Chang YS. Temperature management for the quality assurance of a perishable food supply chain. Food Control, 2014, 40: 198-207.
[7] Mercier S, Villeneuve S, Mondor M, et al. Time–temperature management along the food cold chain: A review of recent developments. Comprehensive Reviews in Food Science and Food Safety, 2017, 16(4): 647-67
[8] Conner DE, Scott VN, Bernard DT, et al. Potential Clostridium botulinum hazards associated with extended shelf-life refrigerated foods: A review. Journal of Food Safety, 1989, 10(2): 131-53.
[9] Kennedy J, Jackson V, Blair IS, et al. Food safety knowledge of consumers and the microbiological and temperature status of their refrigerators. Journal of food protection, 2005, 68(7): 1421-30.
[10] Galos J, Sutcliffe M, Cebon D, et al. Reducing the energy consumption of heavy goods vehicles through the application of lightweight trailers: Fleet case studies. Transportation Research Part D: Transport and Environment, 2015, 41: 40-9.
[11] Siczek K, Siczek K. Modern vehicles for refrigeration. Autobusy: technika, eksploatacja, systemy transportowe, 2018, 19.
[12] Odongkara K, J K O Akumu, M Kyangwa, et al. Survey of the regional fish trade. 2005.
[13] Canals LM, Muñoz I, Hospido A, et al. Life Cycle Assessment (LCA) of domestic vs. imported vegetables. Case studies on broccoli, salad crops and green beans. United Kingdom, Cent. Environ. Strateg. Univ. Surrey, 2008, 46.
[14] Okamoto H, Ide Y, Toyoda M, et al. Refrigerating apparatus for use in vehicles, using an engine as power source. United States patent US 6,688,125. 2004.
[15] Ahmed M, Meade O, Medina MA. Reducing heat transfer across the insulated walls of refrigerated truck trailers by the application of phase change materials. Energy Conversion and Management. 2010 Mar 1;51(3):383-92.
[16] Tassou SA, De-Lille G, Ge YT. Food transport refrigeration–Approaches to reduce energy consumption and environmental impacts of road transport. Applied Thermal Engineering, 2009, 29(8-9): 1467-77.
[17] Barbosa-Cánovas GV, Altunakar B, Mejía-Lorío DJ. Freezing of fruits and vegetables: An agribusiness alternative for rural and semi-rural areas. Food & Agriculture Org, 2005.
[18] Farid MM, Khudhair AM, Razack SA, et al. A review on phase change energy storage: materials and applications. Energy conversion and management, 2004, 45(9-10): 1597-615.
[19] Al-Homoud MS. Performance characteristics and practical applications of common building thermal insulation materials. Building and environment, 2005, 40(3): 353-66.
[20] Baetens R, Jelle BP, Thue JV, et al. Vacuum insulation panels for building applications: A review and beyond. Energy and Buildings, 2010, 42(2): 147-72.
[21] Jelle BP, Gustavsen A, Baetens R. The path to the high performance thermal building insulation materials and solutions of tomorrow. Journal of building physics, 2010, 34(2): 99-123.
[22] Usuki A, Kawasumi M, Kojima Y, et al. Swelling behavior of montmorillonite cation exchanged for ω-amino acids by∈ -caprolactam. Journal of Materials Research, 1993, 8(5): 1174-8.
[23] Lan T, Kaviratna PD, Pinnavaia TJ. Mechanism of clay tactoid exfoliation in epoxy-clay nanocomposites. Chemistry of Materials, 1995, 7(11): 2144-50.

[24] Alexandre M, Dubois P. Polymer-layered silicate nanocomposites: preparation, properties and uses of a new class of materials. Materials science and engineering: R: Reports, 2000, 28(1-2): 1-63.
[25] Kornmann X, Lindberg H, Berglund LA. Synthesis of epoxy–clay nanocomposites. Influence of the nature of the curing agent on structure. Polymer, 2001, 42(10): 4493-9.
[26] Wu H, Liang X, Huang L, et al. The utilization of cotton stalk bark to reinforce the mechanical and thermal properties of bio-flour plastic composites. Construction and Building Materials, 2016, 118: 337-43.
[27] Adekomaya O, Jamiru T, Sadiku R, et al. Sustaining the shelf life of fresh food in cold chain–A burden on the environment. Alexandria Engineering Journal, 2016, 55(2): 1359-1365.
[28] Lyu MY, Choi TG. Research trends in polymer materials for use in lightweight vehicles. International Journal of Precision Engineering and Manufacturing, 2015, 16(1): 213-20.
[29] Zheng WG, Lee YH, Park CB. Use of nanoparticles for improving the foaming behaviors of linear PP. Journal of applied polymer science, 2010, 117(5):2972-9.
[30] De Sciarra FM, Russo P. Experimental Characterization, Predictive Mechanical and Thermal Modeling of Nanostructures and Their Polymer Composites. William Andrew, 2018, 23.
[31] Asadi A, Kalaitzidou K. Process-Structure-Property Relationship in Polymer Nanocomposites. In Experimental Characterization, Predictive Mechanical and Thermal Modeling of Nanostructures and their Polymer Composites Elsevier, 2018: 25-100.
[32] Salamone JC. Concise polymeric materials encyclopedia. CRC press, 1998, 28.
[33] Wang Z, Xiao H. Nanocomposites: recent development and potential automotive applications. SAE International Journal of Materials and Manufacturing, 2009, 1(1): 631-40.
[34] Duguay A. Exfoliated graphite nanoplatelet-filled impact modified polypropylene nanocomposites. Electronic Theses and Dissertations, 2011.
[35] Moraru CI, Panchapakesan CP, Huang Q, et al. Nanotechnology: A New Frontier in Food Science Understanding the special properties of materials of nanometer size will allow food scientists to design new, healthier, tastier, and safer foods. Nanotechnology, 2003, 57(12).
[36] Patel V, Mahajan Y. Polymer nanocomposites: Emerging growth driver for the global automotive industry. InHandbook of polymernanocomposites. Processing, performance and application, Springer, 2014: 511-538.
[37] Szeteiová K. Automotive materials plastics in automotive markets today. Institute of Production Technologies, Machine Technologies, and Materials, Faculty of Material Science and Technology in Trnava, Slovak University of Technology Bratislava. 2010.
[38] Sadiku R, Ibrahim D, Agboola O, et al. Automotive components composed of polyolefins. InPolyolefin Fibres, Woodhead Publishing. 2017: 449-496.
[39] Lyu MY, Choi TG. Research trends in polymer materials for use in lightweight vehicles. International Journal of Precision Engineering and Manufacturing, 2015, 16(1): 213-20.
[40] Stewart R. Automotive composites offer lighter solutions. Reinforced Plastics, 2010, 54(2): 22-8
[41] Park HS, Dang XP, Roderburg A, et al. Development of plastic front side panels for green cars. CIRP Journal of Manufacturing Science and Technology, 2013, 6(1): 44-52.
[42] Sancaktar E, Gratton M. Design, analysis, and optimization of composite leaf springs for light vehicle applications. Composite Structures, 1999, 44(2-3): 195-204.
[43] Gaikwad D, Sonkusare R, Wagh S. Composite leaf spring for lightweight vehicle-materials, manufacturing process, advantages & limitations. International Journal of Engineering and Technoscience, 2012, 3(2): 410-3.
[44] Okada A, Usuki A. Twenty years of polymer-clay nanocomposites. Macromolecular Materials and Engineering, 2006 , 291(12): 1449-76.
[45] Tan B, Thomas NL. A review of the water barrier properties of polymer/clay and polymer/graphene nanocomposites. Journal of Membrane Science, 2016, 514: 595-612.
[46] Ciardelli F, Coiai S, Passaglia E, et al. Nanocomposites based on polyolefins and functional thermoplastic materials. Polymer international, 2008, 57(6): 805-36.
[47] Cui Y, Kumar S, Kona BR, et al. Gas barrier properties of polymer/clay nanocomposites. RSC Advances, 2015, 5(78): 63669-90.
[48] Okamoto M. Recent advances in polymer/layered silicate nanocomposites: an overview from science to technology. Materials Science and Technology, 2006, 22(7): 756-79.
[49] Ma PC, Hao B, Kim JK. Formation and Functionality of Interphase in Polymer Nanocomposites. Interface/Interphase in Polymer Nanocomposites, 2017: 103.
[50] Kiliaris P, Papaspyrides CD. Polymer/layered silicate (clay) nanocomposites: an overview of flame retardancy. Progress in Polymer Science, 2010, 35(7): 902-58.
[51] Manias E, Touny A, Wu L, et al. Polypropylene/montmorillonite nanocomposites. Review of the synthetic routes and materials properties. Chemistry of Materials, 2001, 13(10): 3516-23.
[52] Thabet A, Mubarak YA, Bakry M. A review of nano-fillers effects on industrial polymers and their characteristics. J. Eng. Sci, 2011, 39: 377-403.

[53] DeArmitt C. Applied Minerals Inc, 110 Greene St, Suite 1101. Applied Plastics Engineering Handbook: Processing and Materials, 2011: 455.
[54] Benfarhi, S, Decker, C, Keller, L, et al. Synthesis of clay nanocomposite materials by light-induced crosslinking polymerization. European Polymer Journal, 2004, 40(3): 493-501.
[55] Yasmin A, Abot JL, Daniel IM. Processing of clay/epoxy nanocomposites by shear mixing. Scripts Materialia, 2003, 49(1): 81-86.
[56] Gua B, Jia D, Cai C. Effects of organo-montmorillonite dispersion on the thermal stability of epoxy layered silicate nanocomposites. European Polymer Journal, 2004, 40(8): 1743-1748.
[57] Tolle TB, Anderson DP. Morphology development in layered silicate thermoset nanocomposites. Composites Science and Technology, 2002, 62(7-8): 1033-1041.
[58] Chen C, Khobaib M, Curliss D. Epoxy layered-silicate nanocomposites. Progress in Organic Coatings, 2003, 47(3-4): 376-383.
[59] Maddah HA. Polypropylene as a promising plastic: A review. Am. J. Polym. Sci, 2016, 6(1): 1-1
[60] Müller K, Bugnicourt E, Latorre M, et al. Review on the processing and properties of polymer nanocomposites and nanocoatings and their applications in the packaging, automotive and solar energy fields. Nanomaterials, 2017, 7(4): 74.
[61] Hwang TY, Lee SM, Ahn Y, et al. Development of polypropylene-clay nanocomposite with supercritical CO2 assisted twin screw extrusion. Korea-Australia rheology journal, 2008, 20(4): 235-43.
[62] Sanchez C, Julián B, Belleville P, et al. Applications of hybrid organic-inorganic nanocomposites. Journal of Materials Chemistry, 2005, 15(35-36): 3559-92.
[63] Garcıa-López D, Picazo O, Merino JC, et al. Polypropylene–clay nanocomposites: effect of compatibilizing agents on clay dispersion. European polymer journal, 2003, 39(5): 945-50.
[64] Liu X, Wu Q. PP/clay nanocomposites prepared by grafting-melt intercalation. Polymer, 2001, 42(25): 10013-9.
[65] Prashantha K, Soulestin J, Lacrampe MF, et al. Multi-walled carbon nanotube filled polypropylene nanocomposites based on masterbatch route: Improvement of dispersion and mechanical properties through PP-g-MA addition. Express Polymer Letters, 2008, 2(10): 735-45.
[66] Moncada E, Quijada R, Lieberwirth I, et al. Use of PP grafted with itaconic acid as a new compatibilizer for PP/clay nanocomposites. Macromolecular Chemistry and Physics, 2006, 207(15): 1376-86.
[67] Bikiaris DN, Vassiliou A, Pavlidou E, et al. Compatibilisation effect of PP-g-MA copolymer on iPP/SiO2 nanocomposites prepared by melt mixing. European Polymer Journal, 2005, 41(9): 1965-78.
[68] Zou C, Fothergill JC, Rowe SW. A Water Shell Model for the Dielectric Properties of Hydrated Silica-filled Epoxy Nano-composites. IEEE Intern. Conf. on Solid Dielectr., (ICSD), 2007: 389-392.
[69] Ash BJ, Schadler LS, Siegel RW. Glass transition behavior of Alumina/polymethylmethacrylatenanocomposites. Materials Letters, 2002, 55:83-87.
[70] Mayes AM. Softer at the boundary. Nature Materials, 2005, 4: 651-652.
[71] Eloundou JP. Dipolar relaxations in an epoxy–amine system. Europeans Polymer J, 2002, 38: 431-438.
[72] Nelson JK, Fothergill JC. Internal Charge Behavior of Nanocomposites. Nanotechnology, 2004, 15: 586-595.
[73] Sinha Ray S, Yamada K, Okamoto M, et al. New polylactide/layered silicate nanocomposites. 3. High-performance biodegradable materials. Chemistry of Materials, 2003, 15: 1456-1465.
[74] Sobczak JJ, Drenchev L. Metallic functionally graded materials: a specific class of advanced composites. Journal of Materials Science & Technology, 2013, 29: 297-316.
[75] Soutis C. Carbon fiber reinforced plastics in aircraft construction. Materials Science and Engineering: A, 2005, 412: 171-176.
[76] Khan I, Kamma-Lorger CS, Mohan SD, et al. The Exploitation of Polymer Based Nanocomposites for Additive Manufacturing: A Prospective Review. InApplied Mechanics and Materials, Trans Tech Publications, 2019, 890: 113-145.
[77] Stankovich S, Dikin DA, Piner RD, et al. Synthesis of graphene-based nanosheets via chemical reduction of exfoliated graphite oxide. Carbon, 2007, 45: 1558-1565.
[78] Bhattacharyya, D, Shields R. Modeling of fibre formation and oxygen permeability in micro-fibrillar polymer-polymer composites. IUTAM Symposium on Multi-Functional Material Structures and Systems, Springer, 2010.
[79] Thygesen LG, Løkke MM, Micklander E, et al. Vibrational microspectroscopy of food. Raman vs. FT-IR. Trends in Food Science & Technology, 2003, 14(1-2): 50-7.
[80] Carballo-Meilan A, Goodman AM, Baron MG, et al. A specific case in the classification of woods by FTIR and chemometric: discrimination of Fagales from Malpighiales. Cellulose, 2014, 21(1): 261-73.
[81] Faix O. Fourier transform infrared spectroscopy. InMethods in lignin chemistry. Springer, 1992: 83-109.
[82] Uwa CA, Abe B, Nnachi AF, et al. Experimental investigation of thermal and physical properties of nanocomposites for power cable insulations. Materials Today: Proceedings, 2021, 38: 823-9.
[83] Zhu G, Zhu X, Fan Q, et al. Raman spectra of amino acids and their aqueous solutions. Spectrochimica Acta Part A: Molecular and Biomolecular Spectroscopy, 2011, 78(3): 1187-95.

[84] Noda I, Dowrey AE, Haynes JL, et al. Group frequency assignments for major infrared bands observed in common synthetic polymers. InPhysical properties of polymers handbook. Springer, New York, 2007: 395-406.
[85] Jung MR, Horgen FD, Orski SV, et al. Validation of ATR FT-IR to identify polymers of plastic marine debris, including those ingested by marine organisms. Marine pollution bulletin, 2018, 127: 704-16.
[86] VAIA R A, JANDT K D, KRAMER, E J, et al. Microstructural evolution of melt intercalated polymer− organically modified layered silicates nanocomposites. Chemistry of Materials, 1996, 8: 2628-2635.
[87] TARAPOW J, BERNAL C, ALVAREZ V. Mechanical properties of polypropylene/clay nanocomposites: effect of clay content, polymer/clay compatibility, and processing conditions. Journal of applied polymer science, 2009, 111: 768-778.
[88] Uwa CA, Sadiku ER, Jamiru T, et alF. Synthesis and characterisation of polypropylene nanocomposites for food packaging material. Materials Today: Proceedings, 2021, 38: 1197-202.